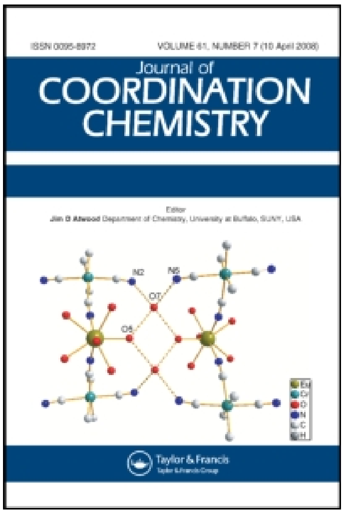

Journal of Coordination Chemistry
Publication details, including instructions for authors and subscription information:
http://www.informaworld.com/smpp/title~content=t713455674

Metal complexes derived from hydrazoneoxime ligands: II. Synthesis, electrospray mass spectra and magnetochemical studies of some copper(II) complexes derived from *p*-substituted aroylhydrazoneoximes

Nahed M. H. Salem[a]; Laila El Sayed[a]; Wolfgang Haase[b]; Magdi F. Iskander[a]
[a] Faculty of Science, Chemistry Department, Alexandria University, Ibrahimia, Alexandria 21321, Egypt [b] Institut fur physikalische Chemie, AG Kondensierte Materie, Fachbereich Chemie, Technische Universitat Darmstadt, Petersenstrasse 20, D-64287 Darmstadt, Germany

To cite this Article Salem, Nahed M. H. , Sayed, Laila El , Haase, Wolfgang and Iskander, Magdi F.(2005) 'Metal complexes derived from hydrazoneoxime ligands: II. Synthesis, electrospray mass spectra and magnetochemical studies of some copper(II) complexes derived from *p*-substituted aroylhydrazoneoximes', Journal of Coordination Chemistry, 58: 15, 1327 — 1343

To link to this Article: DOI: 10.1080/00958970500233255
URL: http://dx.doi.org/10.1080/00958970500233255

Journal of Coordination Chemistry
Vol. 58, No. 15, October 2005, 1327–1343

Taylor & Francis
Taylor & Francis Group

Metal complexes derived from hydrazoneoxime ligands: II. Synthesis, electrospray mass spectra and magnetochemical studies of some copper(II) complexes derived from *p*-substituted aroylhydrazoneoximes

NAHED M. H. SALEM†, LAILA EL SAYED†,
WOLFGANG HAASE‡ and MAGDI F. ISKANDER*†

†Faculty of Science, Chemistry Department, Alexandria University,
P.O. box 426, Ibrahimia, Alexandria 21321, Egypt
‡Institut fur physikalische Chemie, AG Kondensierte Materie,
Fachbereich Chemie, Technische Universitat Darmstadt,
Petersenstrasse 20, D-64287 Darmstadt, Germany

(*Received in final form 3 March 2005*)

Mono- and binuclear copper(II) complexes derived from substituted aroylhydrazoneoximes of the general formulae $[Cu(H_2LR)Cl_2]\cdot nH_2O$, $[Cu(HLR)Cl]$, $[\{Cu(HLR)\}_2]\cdot 2NO_3\cdot nH_2O$ and $[\{Cu(LR)\}_2]\cdot nH_2O$ have been prepared and characterized, where H_2LR, HLR and LR refer, respectively, to the neutral, monoanionic and dianionic ONN tridentate aroylhydrazoneoxime ligands. Electrospray ionization (ESI) mass spectra revealed the formation of tri- and tetranuclear copper(II) complexes in dimethylformamide (DMF) or dimethysulphoxide (DMSO) solutions. The effect of substitution in the aroylhydrazone residue on the degree of deprotonation of the ligand and the energies of d–d transitions of the copper(II) complexes have been studied. Tuning of the antiferromagnetic exchange coupling by different substituents in $[\{Cu(HLR)\}_2]\cdot 2NO_3\cdot nH_2O$ and $[\{Cu(LR)\}_2]\cdot nH_2O$ complexes have been discussed.

Keywords: 2-Hydroxyimino-1-methyl propylidene aroylhydrazines; Copper(II) complexes; Electrospray ionization mass spectra; Magnetic studies; Oximate bridges

1. Introduction

The synthesis and characterization of both mono- and dinuclear copper(II) complexes derived from acylhydrazoneoximes, namely, 2-hydroxyimino-1-methyl propylidene acetyl- and benzoylhydrazine have been previously reported [1]. The stoichiometry and the degree of deprotonation of the acylhydrazoneoxime ligand in these complexes

---

*Corresponding author. Email: m.iskander@link.net

Journal of Coordination Chemistry
ISSN 0095-8972 print: ISSN 1029-0389 online © 2005 Taylor & Francis
DOI: 10.1080/00958970500233255

depend on the copper(II) salts used as well as the pH of the reaction medium. Reactions of acylhydrazoneoximes with copper(II) chloride, nitrate and acetate afforded, respectively, mononuclear dichloro complexes $[Cu(H_2L)Cl_2]$, dinuclear nitrate complexes, $[\{Cu(HL)\}_2]\cdot 2NO_3\cdot nH_2O$ and dinuclear neutral complexes $[\{Cu(L)\}_2]\cdot nH_2O$, where H_2L, HL and L refer, respectively, to neutral, monoanionic and dianionic ONN tridentate acylhydrazoneoxime ligands [1]. Variable temperature magnetic susceptibility measurements for $[Cu(H_2L)Cl_2]$ suggest Curie–Weiss behaviour. However, both $[\{Cu(HL)\}_2]\cdot 2NO_3\cdot nH_2O$ and $[\{Cu(L)\}_2]\cdot nH_2O$ complexes show strong antiferromagnetic exchange coupling with $-2J$ values of 898–934 cm^{-1} and 618–757 cm^{-1}, respectively. A dimeric structure with oximate bridges was proposed for these complexes [1].

In the present article, studies on the coordination chemistry of aroylhydrazoneoximes (figure 1, structure **1**) having different *p*-substituents in the aroylhydrazone residue have been extended. Different types of copper(II) complexes have been prepared and characterized and the electronic effects of the different substituents on both degree of deprotonation of the coordinated aroylhydrazoneoxime ligands and energies of the d–d transitions of the prepared copper(II) complexes will be discussed. Electrospray ionization (ESI) mass spectra will be studied, aiming to identify the different ionic species that may exist in dimethylformamide (DMF) and/or dimethylsulphoxide (DMSO) solutions, and to detect any ionic aggregates with higher nuclearities. Tuning of the antiferromagnetic exchange coupling by different *p*-substituents in the aroylhydrazone residue of the prepared dinuclear copper(II) complexes will be demonstrated and discussed.

2. Experimental

2.1. *Materials*

Aroylhydrazines were prepared by hydrazinolysis of the corresponding methyl esters as previously described [2]. Diacetylmonoxime (Sigma) was used without any further purification.

2.2. *Preparation of aroylhydrazoneoximes (1, R = CH_3, CH_3O, Cl, and NO_2)*

Aroylhydrazoneoximes were prepared according to the procedure previously described for acetyl- and benzoylhydrazoneoximes [1].

H_2LCH_3 (structure **1**, $R = CH_3$): m.p. 217°C. Anal. Calcd for $C_{12}H_{15}N_3O_2$ (%): C, 61.79; H, 6.48; N, 18.01. Found: C, 61.75; H, 6.46; N, 17.98. IR (cm^{-1}): 3333s, ν(OH); 3225m, ν(NH); 1675s, amide I, ν(C=O); 1575m, $\nu(C{=}N)_{hy}$ 1525s $(C{=}N)_{ox}$, 1295s amide III ν(C–N); 1120m, ν(N–O). UV-Vis (EtOH, λ_{max}/nm (log ε)): 234 (4.17), 278 (4.34). ^1H NMR (DMSO-d_6, TMS, ppm): 11.60 (1H, oxime OH), 10.63 (1H, CONH), 7.77 (2H, d, aromatic), 7.27 (2H, d, aromatic), 2.36 (3H, s, CH_3-aromatic), 2.14 (3H, s, $CH_3C{=}NN$), 2.00 (3H, s, $CH_3C{=}NO$). ^{13}C NMR (DMSO-d_6, THS, ppm): 154.71 (C=O), 153.29 (C=N–OH), 141.47 (C=N–NH), 130.97, 128.66, 128.01, 127.04 (aromatic), 20.97 (CH_3-aromatic), 11.72 (CH_3–C=NNH), 9.23 (CH_3–C=NOH). Electron impact/ionization mass spectrometry (EI-MS) (*m*/*z* (RA%)), 233 (9.9), 216 (7), 175 (5.6), 119 (100), 91 (26.8), 65 (12.7).

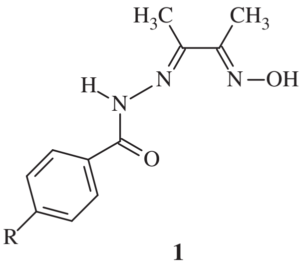

1

H_2LH R = H
H_2LCH_3 R = CH_3
H_2LCH_3O R = CH_3O
H_2LCl R = Cl
H_2LNO_2 R = NO_2

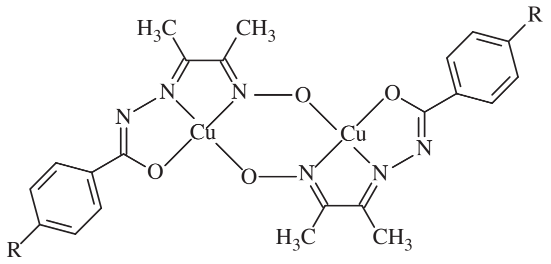

2

R = H
R = CH_3
R = CH_3O
R = Cl
R = NO_2

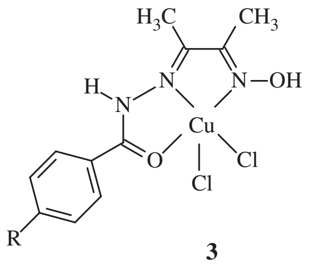

3

R = H
R = CH_3
R = CH_3O
R = Cl

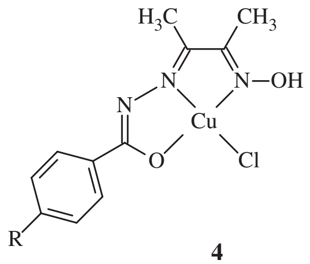

4

R = NO_2

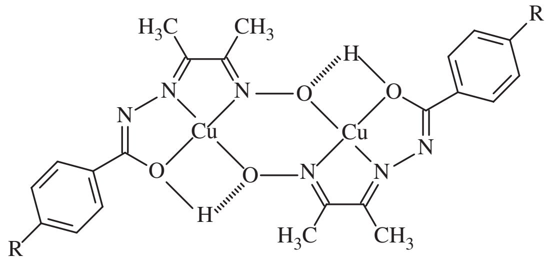

5

R = H
R = CH_3
R = CH_3O

Figure 1. Molecular formulae of 2-hydroxyimino-1-methylpropylidene aroylhydrazines and their copper(II) complexes.

H_2LOCH_3 (structure **1**, R = CH_3O): m.p. 211°C. Anal. Calcd for $C_{12}H_{15}N_3O_3$ (%): C, 57.82; H, 6.07; N, 16.86. Found: C, 57.80; H, 6.02; N, 16.56. IR (cm^{-1}): 3287s ν(OH), 3210m, ν(NH), 1670s amide I ν(C=O), 1550s $\nu(C{=}N)_{hy}$, 1510s $\nu(C{=}N)_{ox}$, 1306s amide III ν(C–N), 1145m ν(N–O). UV-vis (EtOH, λ_{max}/nm ($\log\varepsilon$)): 244 sh, 285 (4.45), ^1H NMR (DMSO-d_6, THS, ppm): 13.50, 12.25 (1H, oxime OH), 11.58, 10.57 (1H, CONH), 7.86 (2H, d, aromatic), 7.00 (2H, d, aromatic), 3.81

(3H, s, CH_3O), 2.17 (3H, s, $CH_3C{=}NN$), 2.00 (3H, s, $CH_3C{=}NO$). ^{13}C NMR (DMSO-d_6, THS, ppm): 161.74 (C=O), 154.79 (2C=N), 130.02, 125.79, 113.33 (aromatic) 55.30 (CH_3O), 11.62 (CH_3–C=NNH), 9.21 (CH_3–C=NOH). EI-MS (*m*/*z* (RA%)), 249 M^+ (15.2), 191 (6), 135 (100), 107 (18.5), 92 (19.2), 77 (33.8), 64 (9.9).

H_2LCl (structure **1**, R = Cl): m.p. 205°C. Anal. Calcd for $C_{11}H_{12}N_3O_2Cl$ (%): C, 52.08; H, 4.77; N, 16.56. Found: C, 52.01; H, 4.43; N, 16.32. IR (cm^{-1}): 3445m, 3285s ν(OH), 3200m ν(NH), 1660s amide I, ν(C=O), 1570s $\nu(C{=}N)_{hy}$, 1535s $\nu(C{=}N)_{ox}$, 1275s amide III, ν(C–N), 1145m ν(N–O). UV-vis (EtOH, λ_{max}/nm (log ε)): 234 (4.17), 280 (4.22). ^1H NMR (DMSO-d_6, THS, ppm): 11.63 (1H, oxime OH), 10.80 (1H, CONH), 7.86 (2H, d, aromatic), 7.57 (2H, d, aromatic), 2.14 (3H, s, $CH_3C{=}NN$), 2.00 (3H, s, $CH_3C{=}NO$). EI-MS (*m*/*z* (RA%)), 253 M^+ (10.7), 236 (11.3), 195 (8), 139 (100), 114 (41.3), 75 (8.7).

H_2LNO_2 (structure **1**, R = NO_2): m.p. 201°C. Anal. Calcd for $C_{11}H_{12}N_4O_4$ (%): C, 50.00; H, 4.58; N, 21.20. Found: C, 49.96; H, 4.52; N, 21.11. IR (cm^{-1}): 3304m ν(OH); 3190m ν(NH); 1670s amide I, ν(C=O); 1600s $\nu(C{=}N)_{hy}$; 1525m $\nu(C{=}N)_{ox}$; 1288s amide III, ν(C–N); 1150m ν(N–O). UV-vis (EtOH, λ_{max}/nm (log ε)): 253 (4.29), 295sh, ^1H NMR (DMSO-d_6, THS, ppm): 11.70, 11.55 (1H, oxime OH), 11.06 (1H, CONH), 8.57 (2H, d, aromatic), 8.08 (2H, d, aromatic), 2.19 (3H, s, $CH_3C{=}NN$), 2.05 (3H, s, $CH_3C{=}NO$). EI-MS (*m*/*z* (RA%)), 264 (12.5), 247 (16.4), 206 (13.8), 181 (37.5), 164 (40.1), 150 (100), 114 (45.4), 104 (77), 92 (32.2), 76 (57.2), 69 (12.5).

2.3. *Preparation of copper(II) complexes*

2.3.1. Preparation of [{Cu(LR)}$_2$]·nH$_2$O (2, R = H, CH$_3$, CH$_3$O, Cl and NO$_2$). To a solution of aroylhydrazoneoxime (**1**, R = H, CH_3, CH_3O, Cl or NO_2) (1.0 mmol) in methanol (30 cm^3), a solution of copper(II) acetate monohydrate (1.0 mmol) was added. The resulting mixture was treated with a solution of KOH (2.0 mmol) in methanol (20 cm^3). The reaction mixture was then boiled under reflux with constant stirring for 3 h. The isolated complex was filtered while hot, washed with boiling methanol then dried *in vacuo*. The elemental analyses of the prepared copper(II) complexes, $[\{Cu(L\text{-}R)\}_2]\cdot nH_2O$, are listed in table 1.

2.3.2. Preparation of [Cu(H$_2$LR)Cl$_2$]·nH$_2$O (3, R n = H, CH$_3$, CH$_3$O and Cl). A solution of aroylhydrazonemonoxime (**3**, R = H, CH_3, CH_3O or Cl) (1.0 mmol) in absolute ethanol (40 cm^3) was added to a solution of copper(II) chloride dihydrate (1.0 mmol) in absolute ethanol (30 cm^3). The reaction mixture was stirred at room temperature for about 2 h. The isolated chloro complex was filtered, washed with absolute ethanol then dried *in vacuo*. The isolated $[Cu(H_2L\text{-}R)Cl_2]\cdot nH_2O$ complexes together with their elemental analyses are also included in table 1.

2.3.3. Preparation of [Cu(HLNO$_2$)Cl]·1/2H$_2$O (4, R = NO$_2$). This complex was isolated from the reaction of diacetyl *p*-nitrobenzoylhydrazone monoxime (**1**, R = NO_2) with copper(II) chloride dihydrate using the same procedure described for $[Cu(H_2L\text{–}R)Cl_2]\cdot 1/2H_2O$ complexes. Elemental analysis (table 1) is in agreement with the formation of monochloro rather than the dichloro copper(II) complex.

Table 1. Elemental analyses of copper(II) complexes derived from aroylhydrazoneoximes.

Complex			Found (Calcd) (%)		
R	*n*	Yield (%)	C	H	N
$[\{CuLR\}_2]\cdot nH_2O$					
CH_3	2	73	46.18 (46.08)	4.69 (4.83)	13.23 (13.43)
CH_3O	1	72	44.85 (45.07)	4.38 (4.41)	12.88 (13.14)
Cl	2	75	39.40 (39.65)	3.67 (3.63)	12.60 (12.61)
NO_2	3	75	37.94 (37.71)	3.53 (3.71)	15.79 (15.88)
$[Cu(H_2LR)Cl_2]\cdot nH_2O$					
CH_3	1	60	37.15 (37.37)	4.52 (4.44)	10.68 (10.89)
CH_3O	–	60	37.15 (37.56)	3.92 (3.93)	10.54 (10.95)
Cl	1	63	32.77 (32.53)	3.47 (3.47)	10.02 (10.35)
$[Cu(HLR)Cl]\cdot nH_2O$					
NO_2	0.5	48	35.73 (35.59)	3.25 (3.26)	14.94 (15.09)
$[\{Cu(HLR)\}_2](NO_3)_2\cdot nH_2O$					
CH_3	4	49	36.60 (36.48)	4.31 (4.61)	14.38 (14.23)
CH_3O	2	52	36.62 (36.78)	4.41 (4.12)	14.12 (14.30)

2.3.4. Preparation of $[\{Cu(HLR\}_2]\cdot 2NO_3\cdot nH_2O$ (5, R = H, CH_3 and CH_3O). A solution of copper(II) nitrate trihydrate (1.0 mmol) in ethanol (20 cm^3) was added dropwise with constant stirring to a solution of aroylhydrazone oxime (**1**, R = H, CH_3, or CH_3O) (1.0 mmol) in ethanol (30 cm^3). The reaction mixture was stirred at room temperature for 3 h and the formed complex was filtered, washed with ethanol then dried *in vacuo*.

2.4. *Physical measurements*

The infrared spectra were recorded on a Perkin–Elmer 1430 Data system and/or a Perkin–Elmer (FT-IR) Paragon 1000 PC spectrophotometer. Calibrations of frequency reading were made with polystyrene film. Solid samples were examined as KBr discs. The ultraviolet (UV) and visible (vis) absorption spectra were recorded on double beam ratio recording Lambda 4B Perkin–Elmer spectrophotometers. ^1H and ^{13}C NMR were recorded on Brucker WM 300 (300 MHz) instrument. Mass spectra were recorded on Esquire-LC from Bruker Daltonic Nebulizer 10 psi (dry gas 8 L min^{-1}, dry temperature 250°C). Theoretical isotopic distribution patterns for ionic species were generated using ISOFORM program and/or Sheffield University Chemputer software [3]. Magnetic susceptibilities of powdered dried samples were recorded on a Faraday-type magnetometer using a sensitive computer controlled D-200 Cahn RG microbalance in the temperature range 4.4–300 K. The magnetic field applied was $\sim$1.5 T. Details of the apparatus have been described elsewhere [4, 5]. Experimental susceptibility data were corrected for the underlying diamagnetism using Pascal's constants [6].

3. Results and discussion

3.1. *Synthesis*

Condensation of diacetylmonoxime and aroylhydrazines $NH_2NHCOC_6H_4R$ (R = H, CH_3, CH_3O, Cl and NO_2) in ethanol afforded the corresponding aroylhydrazoneoxime (figure 1, structure **1**, hereafter abbreviated as H_2LR). The purity of the isolated aroylhydrazoneoximes was checked by elemental analysis, EI mass spectra as well as ^1H and ^{13}C NMR spectra.

In the presence of KOH, reaction of H_2LR with copper(II) acetate using 1 : 1 molar ratio in methanol resulted in the deprotonation of both oxime and aroylhydrazone protons and afforded the neutral dimeric complexes $[\{CuLR\}_2] \cdot nH_2O$ as shown in figure 1 (structure **2**, R = H, CH_3, CH_3O, Cl and NO_2). The isolated $[\{CuLR\}_2] \cdot nH_2O$ complexes are insoluble in both hydroxylic and non-polar solvents, but show limited solubility in DMF and DMSO. Attempts to isolate crystals suitable for X-ray diffraction were unsuccessful.

Although a number of bisligand copper(II) complexes of the type $[Cu(HLR)_2]$ were previously reported [7, 8], attempts to prepare bisligand complexes by using two equivalents of aroylhydrazoneoxime, under the same experimental conditions, were unsuccessful and only $[\{CuLR\}_2] \cdot nH_2O$ complexes were obtained.

Reaction of H_2LR (**1**, R = H, CH_3, CH_3O, Cl) with $CuCl_2 \cdot 2H_2O$ in ethanol, using (1 : 1) molar ratio, proceeded with the formation of the monomeric dichloro complexes $[Cu(H_2LR)Cl_2] \cdot nH_2O$ (structure **3**, R = H, CH_3, CH_3O, Cl). However, the reaction of aroylhydrazoneoxime with strong electron withdrawing p-NO_2 substituent (**1**, R = NO_2) in ethanol gave the monochloro complex $[Cu(HLNO_2)Cl] \cdot 1/2H_2O$ as shown in figure 1 (structure **4**, R = NO_2). However, the reaction of copper(II) nitrate with H_2LR (**1**, H, CH_3 and CH_3O) proceeded with the deprotonation of the aroylhydrazone residue and eventually gave the corresponding dimeric copper(II) nitrate complexes $[\{Cu(HLR)\}_2] \cdot 2NO_3 \cdot nH_2O$ (structure **5**, R = H, CH_3 and CH_3O). Different from aroylhydrazoneoximes with electron releasing substituents, the reaction of aroylhydrazoneoximes with electron withdrawing substituents (structure **1**, R = Cl and NO_2) with copper(II) nitrate afforded the dimeric neutral copper(II) complexes $[\{CuLR\}_2] \cdot nH_2O$ similar to that isolated from the reaction with copper(II) acetate.

3.2. *Electrospray ionization (ESI) mass spectra*

The positive ion ESI mass spectra of the dinuclear neutral copper(II) complexes $[\{Cu(LR)\}_2]$ (R = H, CH_3, CH_3O, Cl and NO_2) in slightly acidified DMSO or DMF, table 2, show the most intense peaks (RI = 100%) corresponding to the dimeric monoprotonated cations $[\{Cu(LR)\}_2 + H^+]^{1+}$ besides less intense peaks corresponding to the diprotonated species $[\{Cu(LR)\}_2 + 2H^+]^{2+}$. This confirms the stability of the dimeric structure in these coordinating solvents. Apart from the p-nitro derivative, the ESI mass spectra also show two groups of peaks corresponding to monoprotonated trinuclear $[\{Cu(LR)\}_3 + H^+]^{1+}$ (R = H, CH_3 and CH_3O), and tetranuclear $[\{Cu(LR)\}_4 + H^+]^{1+}$ species (R = H, CH_3, CH_3O and Cl) as shown in table 2.

The positive ESI mass spectra of the dichloro complexes $[Cu(H_2LR)Cl_2]$ in DMF and/or DMSO reveal that these complexes are labile and can undergo varieties of reactions, namely: (i) dissociation, (ii) deprotonation, (iii) disproportionation as well as aggregate formation as shown in figure 2. The ESI mass spectra show the most abundant peaks corresponding to the intact molecular ion $[Cu(HLR)]^{1+}$ (R = CH_3, CH_3O and Cl) which is formed in solution via successive dissociation, deprotonation then desolvation of the parent $[Cu(H_2LR)Cl_2]$. The spectra also show prominent peaks due to the monoprotonated bisligand cation $[Cu(HLR)_2 + H^+]^{1+}$ generated in solution from the disproportionation of $[Cu(HLR)]^{1+}$. Deprotonation of $[Cu(HLR)]^{1+}$ leads to

Table 2. ESI mass spectra of copper(II) complexes derived from aroylhydrazoneoximes.

Complex					
R	*n*	Solvent	*M*/*z* (RI %)	Assignment	*m*/*z* (Calcd)
$[\{Cu(L\text{-}R)\}_2]\cdot nH_2O$					
H	1	DMSO	282.1 (6.5)	$[\{Cu(LH)\}_2+2H^+]^{2+}$	281.7807
			562.3 (100)	$[\{Cu(LH)\}_2+H^+]^{1+}$	562.5536
			843.0 (3.1)	$[\{Cu(LH)\}_3+H^+]^{1+}$	843.2264
			1124.0 (8.4)	$[\{Cu(LH)\}_4+H^+]^{1+}$	1124.0991
CH_3	2	DMSO	295.3 (8.9)	$[\{Cu(LCH_3)\}_2+2H^+]^{2+}$	295.8075
			590.2 (100)	$[\{Cu(LCH_3)\}_2+H^+]^{1+}$	590.6070
			885.2 (3.4)	$[\{Cu(LCH_3)\}_3+H^+]^{1+}$	885.4067
			1179.1 (14.6)	$[\{Cu(LCH_3)\}_4+H^+]^{1+}$	1180.2063
CH_3O	1	DMSO	468.3 (13.5)	$[Cu(LOCH_3)(DMSO)_2+H^+]^{1+}$	468.0766
			622.1 (100)	$[\{Cu(LOCH_3)\}_2+H^+]^{1+}$	622.6058
			699.0 (4.5)	$[\{Cu(LOCH_3)\}_2(DMSO)+H^+]^{2+}$	700.7409
			1244.0 (5.6)	$[\{Cu(LOCH_3)\}_4+H^+]^{2+}$	1244.204
Cl	2	DMF	318.2 (17.8)	$[\{Cu(LCl)\}_2+2H^+]^{2+}$	316.2259
			631.0 (100)	$[\{Cu(LCl)\}_2+H]^{1+}$	631.4436
			667.0 (5.2)	$[\{Cu(LCl)\}_4(DMF)+2H^+]^{2+}$	667.9909
			1262.0 (3.0)	$[\{Cu(LCl)\}_4+H]^{1+}$	1261.880
NO_2	3	DMF	326.5 (1.0)	$[\{Cu(LNO_2)\}_2+2H^+]^{2+}$	326.7783
			360.0 (16.7)	$[\{Cu(LNO_2)\}_2\ (DMF)+2H^+]^{2+}$	363.3255
			651.1 (100)	$[\{Cu(LNO_2)\}_2+H^+]^{1+}$	652.5488
$[Cu(H_2L\text{-}R)Cl_2]\cdot nH_2O$					
CH_3	1	DMSO	296.1 (100)	$[Cu(HLCH_3)]^{1+}$	295.8075
			528.2 (20.0)	$[Cu(HLCH_3)_2+H^+]^{1+}$	529.0769
			589.1 (30.3)	$[\{Cu(LCH_3)\}_2+H^+]^{+}$	590.6070
			815.0 (9.0)	$[\{Cu(HLCH_3)Cl\}_2(DMSO)+H^+]^{1+}$	817.7828
			884.1 (9.0)	$[\{Cu(LCH_3)\}_3+H^+]^{1+}$	885.4067
			1104.0 (6.2)	$[\{Cu(H_2LCH_3)Cl_2+H^+]^{1+}$	1104.1722
CH_3O	–	DMSO	312.1 (64.0)	$[Cu(HLOCH_3)]^{1+}$	311.8070
			560.3 (84.3)	$[Cu(HLOCH_3)_2+H^+]^{1+}$	561.0757
			623.1 (100)	$[\{Cu(LOCH_3)\}_2+H^+]^{1+}$	622.6058
			658.0 (6.5)	$[\{Cu(HLOCH_3)\}_2Cl]^{1+}$	659.0669
			694.2 (6.5)	$[\{Cu(HLOCH_3)Cl\}_2+H^+]^{1+}$	696.5278
			933.0 (5.5)	$[\{Cu(LOCH_3)\}_3+H^+]$	933.4050
Cl	1	DMF	316.0 (100)	$[\{Cu(HLCl)\}_2]^{2+}$	316.2258
			334.0 (20.7)	$[\{Cu(HLCl)\}_2Cl+H^+]^{2+}$	334.4563
			351.0 (18.5)	$[\{Cu(HLCl)Cl\}+H^+]^{1+}$	352.6867
			462.0 (7.0)	$[\{Cu(H_2LCl)Cl_2\cdot DMF\}+H^+]^{1+}$	462.2421
			569.0 (75.8)	$[Cu(HLCl)_2+H^+]^{1+}$	569.9134
			604.0 (15.0)	$[Cu(H_2LCl)_2Cl]^{1+}$	606.3744
			630.0 (11.6)	$[\{CuL\}_2+H^+]^{1+}$	631.4436
$[\{Cu(HL\text{-}R)\}_2]\cdot 2NO_3\cdot nH_2O$					
H		DMF	281.2 (11.0)	$[Cu(HL\text{-}H)]^{1+}$	281.7807
			500.7 (17.3)	$[Cu(HL\text{-}H)_2+H^+]^{1+}$	501.0233
			562.2 (100.0)	$[\{Cu(L\text{-}H)\}_2+H^+]^{1+}$	562.5536
			843.0 (30.2)	$[\{Cu(L\text{-}H)\}_3+H^+]^{1+}$	843.3264
			1124.0 (2.5)	$[\{Cu(L\text{-}H)\}_4+H^+]^{1+}$	1124.0991
CH_3	4	DMF	296.0 (15.0)	$[\{Cu(HL\text{-}CH_3)\}_2]^{2+}$	295.8075
			529.0 (14.2)	$[Cu(HL\text{-}CH_3)_2+H^+]^{1+}$	529.0769
			590.0 (100.0)	$[\{Cu(L\text{-}CH_3)\}_2+H^+]^{1+}$	590.6070
			885.0 (22.2)	$[\{Cu(L\text{-}CH_3)\}_3+H^+]^{1+}$	885.4064
			1180.0 (2.0)	$[\{Cu(L\text{-}CH_3)\}_4+H^+]^{1+}$	1180.2063
CH_3O	2	DMF	311.2 (9.5)	$[\{Cu(HL\text{-}CH_3O)\}_2]^{2+}$	311.8069
			560.4 (15.1)	$[Cu(HL\text{-}CH_3O)_2+H^+]^{1+}$	561.0757
			621.4 (100.0)	$[\{Cu(L\text{-}CH_3O)\}_2+H^+]^{1+}$	622.6058
			933.1 (31.5)	$[\{Cu(L\text{-}CH_3O)\}_3+H^+]^{1+}$	933.4050
			1243.0 (3.0)	$[\{Cu(L\text{-}CH_3O)\}_4+H^+]^{1+}$	1244.2040

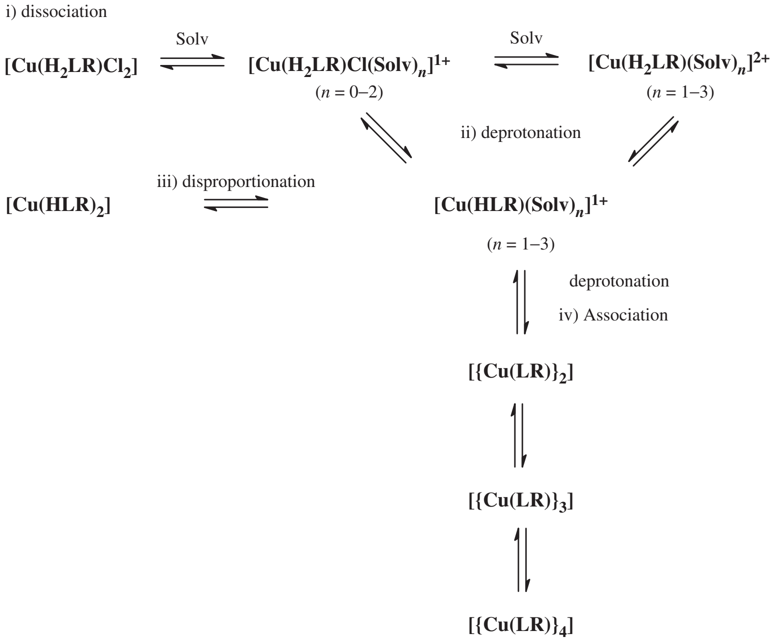

Figure 2. Schematic representation of different equilibria in DMSO and/or DMF solutions of $[Cu(H_2LR)Cl_2]$.

the simultaneous formation of the neutral dimeric $[\{Cu(LR)\}_2]$ and trimeric species $[\{Cu(LR)\}_3]$ ($R = CH_3$, CH_3O). This is evident from the observed two groups of peaks corresponding to the monoprotonated cations $[\{Cu(LR)\}_2 + H^+]^{1+}$ and $[\{Cu(LR)\}_3 + H^+]^{1+}$ respectively. The spectrum of the chloro substituted complex shows peaks corresponding only to dimeric species and no peaks due to trinuclear species were detected.

Similar to the ESI mass spectra of neutral dinuclear complexes, the spectra of the nitrate complexes $[\{Cu(HLR)\}_2] \cdot 2NO_3$ ($R = H$, CH_3 and CH_3O) in DMF show the most intense peaks ($RI = 100\%$) corresponding to the monoprotonated dimeric cation $[\{Cu(LR)\}_2 + H^+]^{1+}$ rather than $[Cu(HLR)]^{1+}$ which dominates the spectra of the corresponding dichloro complexes, thus confirming the dimeric nature of the nitrate complexes. The spectra also display two groups of peaks due to monoprotonated tri- and tetranuclear cations. The experimental and calculated isotope distribution patterns for $[\{Cu(LCH_3O)\}_2 + H^+]^{1+}$ and $[\{Cu(LCH_3O)\}_3 + H^+]^{1+}$ are shown in figure 3.

Similar to that observed in the spectra of dichloro complexes, the spectra of the nitrate complexes display peaks corresponding to bisligand cation $[Cu(HLR)_2 + H^+]^{1+}$, the observed isotope distribution pattern recorded for $[Cu(HLR)_2 + H^+]^{1+}$ together with the calculated pattern is shown in figure 4. Both tri- and tetranuclear species may be either generated during the ionization process or may exist in equilibrium with the dinuclear species. The isolation and characterization of many cyclic tri- [9] and tetranuclear copper(II) complexes [10] with oximate bridges favour the later possibility, and the existence of both tri- and tetranuclear species in the original solution may be more feasible.

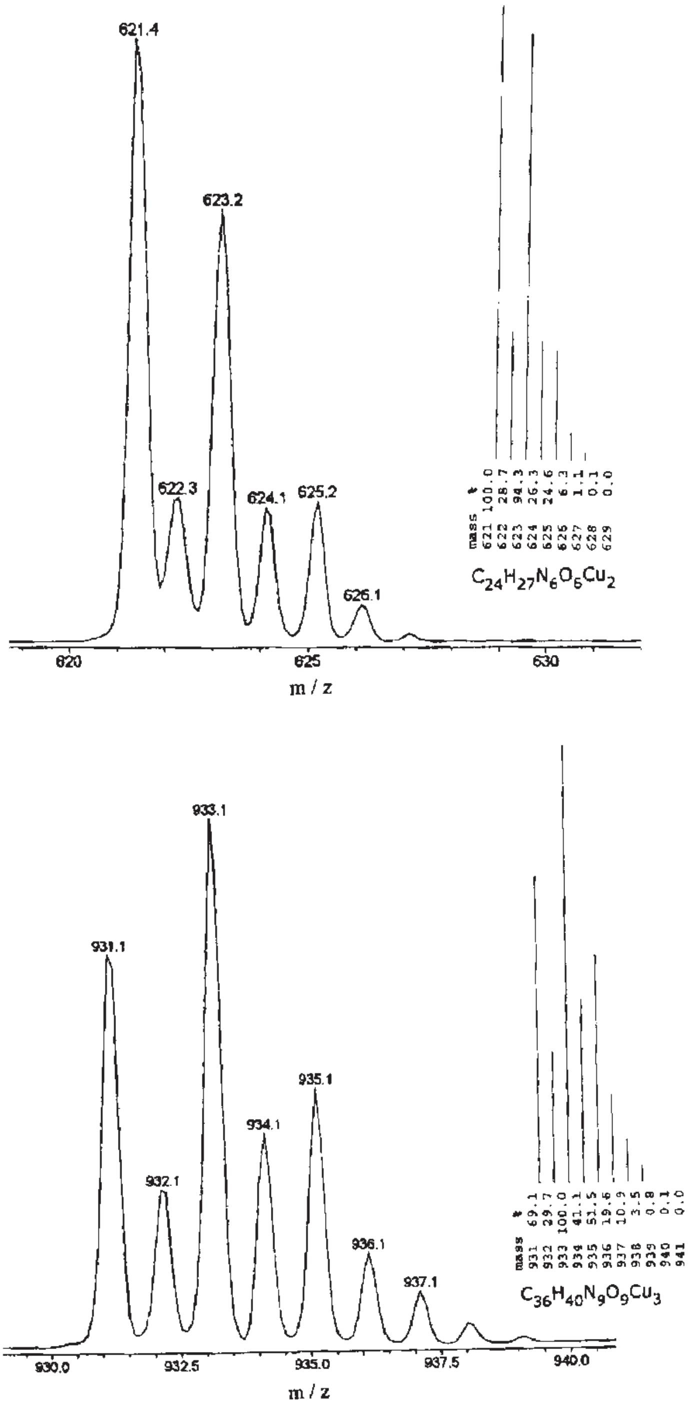

Figure 3. Observed and calculated isotopic mass distribution for $[\{Cu(LCH_3O)\}_2 + H^+]^{1+}$ and $[\{Cu(LCH_3O)_3\} + H^+]^{1+}$ ions in the ESI mass spectrum of $[\{Cu(HLCH_3O)_2\}] \cdot 2NO_3$.

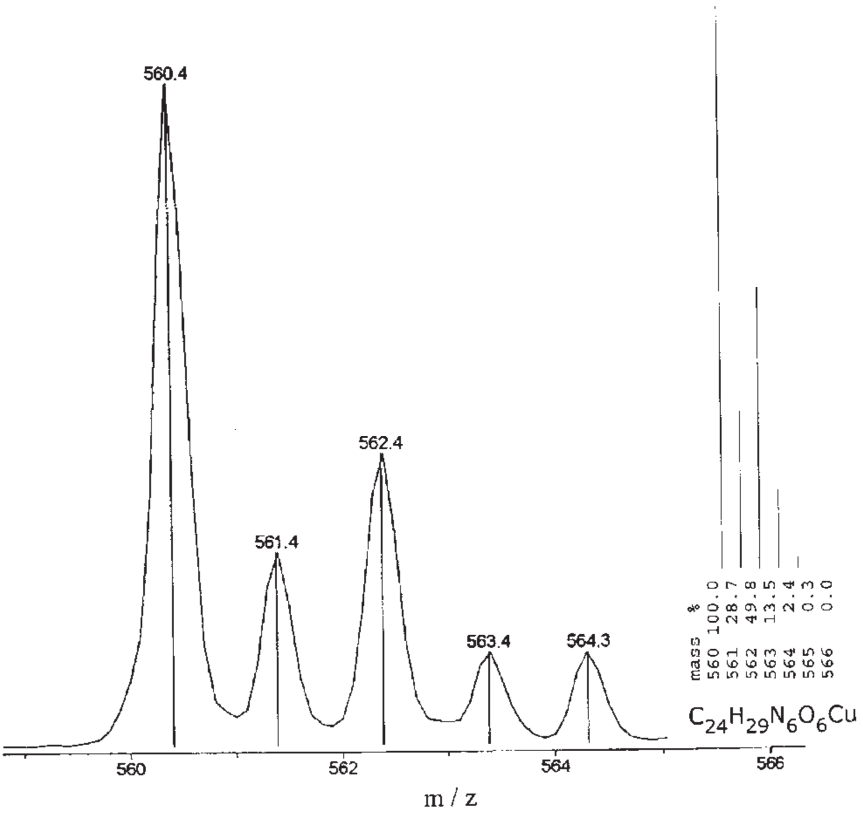

Figure 4. Observed and calculated isotopic mass distribution for $[Cu(LCH_3O)_2 + H^+]^{1+}$ in the ESI mass spectrum of $[\{Cu(LCH_3O)\}_2] \cdot 2NO_3$.

3.3. *Infrared spectra*

The significant IR absorption bands of the prepared copper(II) complexes are listed in table 3. Spectra of the dichloro complexes $[Cu(H_2LR)Cl_2]$ (figure 1, structure **3**, R = CH_3, CH_3O and Cl), display a series of bands due to ν(N–H), amide I [ν(C=O)], $\nu(C{=}N)_{hy}$, and amide III [ν(C–N)] of the aroylhydrazone residue besides the ν(O–H), $\nu(C{=}N)_{ox}$ and ν(N–O) of the hydroxyimino group. The amide I [ν(C=O)], $\nu(C{=}N)_{hy}$, $\nu(C{=}N)_{ox}$ and ν(N–O) are shifted to lower frequencies while the ν(C–N) absorptions are shifted to higher frequencies relative to those of the parent free ligands, suggesting that the aroylhydrazoneoxime ligand in these complexes acts as a neutral NNO tridentate ligand as shown in figure 1 (structure **3**, R = CH_3, CH_3O and Cl). Different from the IR spectra of the dichloro complexes, the spectrum of the monochloro complex $[Cu(HLNO_2)Cl]$ (figure 1, structure **4**, R = NO_2), lacks absorptions due to ν(N–H) and amide I [ν(C=O)], but shows intense absorption at ca. 1600–1610 cm^{-1} due to ν(C=N–N=C) indicating the deprotonation of the enolimine form of the aroylhydrazone residue. The formation of the monochloro complex $[Cu(HLNO_2)Cl]$ rather than the expected $[Cu(H_2LNO_2)Cl_2]$ is attributed to the presence of electron-withdrawing *p*-NO_2 group in the aroylhydrazone residue which facilitates the deprotonation of the enolimide group while the oxime residue remains protonated.

Table 3. Significant bands in the IR spectra of aroylhydrazoneoximes and their copper(II) complexes.

Compound R	ν(OH)	ν(NH)	Amide I ν(C=O)	ν(C=N–N=C)	$\nu(C{=}N)_{hy}$ ν(C=C)	$\nu(C{=}N)_{ox}$	Amide III	ν(N–O)
H_2LR								
H	3328s	3270m	1640s	–	1615s, 1580s	1530s	1290s	1140m
CH_3	3333s	3225m	1675s	–	1610s, 1575s	1525s	1295s	1120m
CH_3O	3287s	3210m	1670s	–	1605s, 1550m	1510s	1306s	1145m
Cl	3445m, 3285s	3200m	1660s	–	1595s, 1570s	1535s	1275s	1145m
NO_2	3304m	3190m	1670s	–	1600s	1525m	1288s	1150m
$[\{Cu(LR)\}_2]\cdot nH_2O$								
H	–	–	–	1618s	1595s, 1550s, 1535s	1505s	1300s	1160m
CH_3	–	–	–	1607s	1578m, 1550m, 1532m	1500s	1330s	1130m
CH_3O	–	–	–	1602s	1575s	1495s	1320s	1121m
Cl	–	–	–	1595m	1578m, 1550m	1515m	1327s	1130m
NO_2	–	–	–	1607s	1570m, 1550m	1527m	1320s	1133m
$[Cu(H_2LR)Cl_2]\cdot nH_2O$								
H	3285m	3195m	1610s	–	1595s	1525s	1300s	1165m
CH_3	3440m	3280	1605s	–	1597s, 1560s	1527s	1310s	1127m
CH_3O	3380s	3130	1605s	–	1590s, 1560, 1525	1505s	1320s	1130m
Cl	3368s		1600s	–	1590s, 1555, 1525	1523s	1315s	1125m
$[\{Cu(HLR)\}_2]\cdot 2NO_3\cdot nH_2O$								
H	3385s	–	–	1610s	1570, 1540	1510s	1325s	1127m
CH_3	3390s	–	–	1610s	1565, 1540	1510s	1330s	1130m
CH_3O	3555s, 3385	–	–	1606s	1562, 1537	1502s	1330s	1125m

Spectra of the neutral complexes [{Cu(LR)}$_2$] (figure 1, structure **2**, R = H, CH_3, CH_3O, Cl and NO_2), lack absorption bands due to ν(O–H), ν(N–H), amide I [ν(C=O)], amide II [δ(N–H)], but display absorptions due to ν(C=N–N=C) and $\nu(C{=}N)_{ox}$, respectively at ca. 1610 and 1500–1525 cm^{-1}. The spectra indicate the deprotonation of both aroylhydrazone and oxime residues and suggest the coordination of the hydrazone ligand via the azomethine hydrazine nitrogen, the deprotonated enolized carbonyl oxygen and the deprotonated oxime group.

Spectra of the nitrate complexes, also lack absorptions due to ν(N–H), amide I [ν(C=O)], amide II [δ(N–H)], but show an intense absorption at ca. 1610 cm^{-1} due to ν(C=N–N=C) indicating the deprotonation of the enolimine form of the aroylhydrazone residue, while the oxime group remains protonated. As previously reported [1], structure **5** (figure 1) can be proposed for these nitrate [{Cu(HLR)}$_2$] $\cdot$ 2NO_3 $\cdot$ $n$$H_2O$ (R = CH_3 and CH_3O) complexes.

3.4. *Ultraviolet-visible (UV-vis) spectra*

The solution absorption spectra of the copper(II) complexes in DMF (table 4) show absorption bands due to d–d, LMCT and intraligand transitions. The d–d bands of neutral dicopper(II) complexes, [{Cu(LR)}$_2$], appear at ca. 580–650 nm suggesting square planar environment with a $^2B_{1g}$ ground state [11]. It is apparent from the data given in table 4 that the position of d–d bands is affected by the nature of *p*-substituents in the aroylhydrazone residue. The energy of the d–d bands, measured in wavenumber (in cm^{-1}), can be correlated with Hammett's σ_p constants and plot of wavenumber against σ_p gave a straight line with a negative slope as shown in figure 5. This linear relation indicates that in these neutral dicopper(II) complexes the ligand field band positions are determined mainly by the electron densities on the ligand donor atoms. On increasing σ_p (increasing substituents electronegativity) less electron densities are localized on the donor atoms, thus decreasing the ligand field strength and the d–d

Table 4. Solution electronic absorption spectra of aroylhydrazoneoxime copper(II) complexes in DMF.

	λ_{max}(nm)(log ε)		
Complex R	L–L*	LMCT	d–d
[{Cu(LR)}$_2$] $\cdot$ nH$_2$O			
H^a	390		590
CH_3^{a}	390	440sh	585
CH_3O^{a}	390	450sh	580
Cl^a	390	440sh	600
NO_2^{a}	404	440sh	645
[Cu(H$_2$LR)Cl$_2$] $\cdot$ nH$_2$O			
H	385 (4.05)	430 sh	660sh, 850 (1.97)
CH_3	390 (4.01)	438sh	675sh, 865 (1.95)
CH_3O	390 (4.05)	435sh	655sh, 875 (1.86)
Cl	390 (4.09)	437sh	655sh, 860 (1.88)
[Cu(HLR)Cl] $\cdot$ nH$_2$O			
NO_2	404 (4.12)	440sh	655sh, 740 (2.07)
[{Cu(HLR)}$_2$] $\cdot$ 2NO$_3$ $\cdot$ nH$_2$O			
H	385 (4.10)	430sh	650 (2.20)
CH_3	390 (4.07)	440sh	655 (2.14)
CH_3O	390 (4.15)	435sh	655 (2.10)

^{a} Saturated solution.

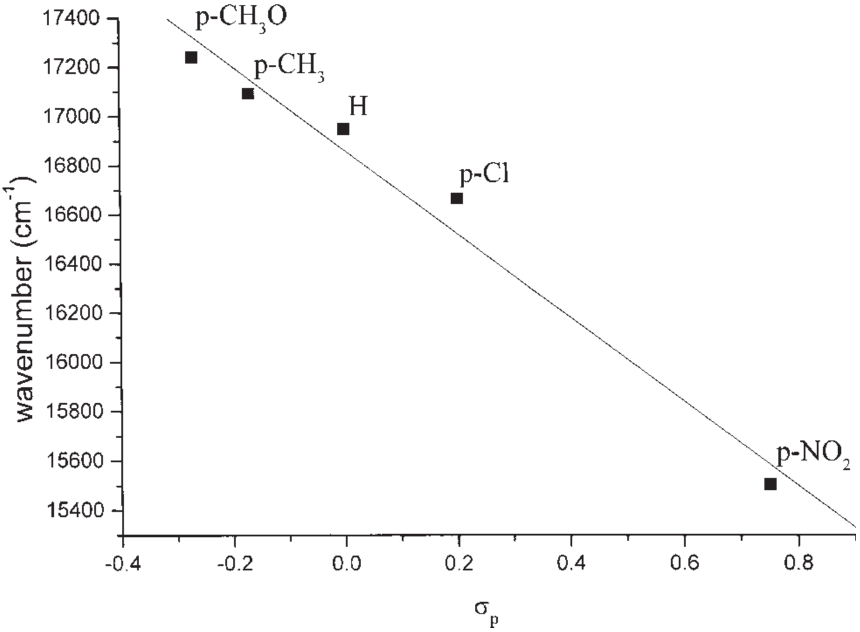

Figure 5. Plot of wavenumber (in cm^{-1}) of d–d transitions for neutral dimeric complexes, [{Cu(LR)$_2$}], against σ_p.

bands suffer a red shift. This behaviour indicates the domination of metal–ligand σ-interactions.

The d–d spectra of monomeric dichloro complexes show a broad absorption band at ca. 860 nm with a shoulder at higher energy side (ca. 650 nm). The spectra suggest the formation of octahedral solvated $[Cu(H_2LR)(DMF)_3]^{2+}$ in equilibrium with $[Cu(H_2LR)(DMF)_2]^{2+}$ species [11]. Introducing either electron releasing (**3**, R = CH$_3$O and CH$_3$) or electron withdrawing substituents (**3**, R = Cl) in the dichloro complexes shift the longer wavelength d–d band to lower energies as shown in figure 6. This behaviour indicates that in these octahedral species both $(L \rightarrow M)\sigma$ and $(L \rightarrow M)\pi$ interactions are operating. The extents of these two competing interactions depend on the nature of substituents which in its turn can affect the relative energies of the ligand σ and π orbitals [12]. In complexes with electron releasing substituents, $(L \rightarrow M)\pi$ interaction seems to dominate and the t_{2g} level is destabilized, thus Δ_0 is decreased relative to that of the unsubstituted dichloro complex. Electron withdrawing substituents, however, can promote the $(L \rightarrow M)\sigma$ interaction and the resulted decrease in electron densities on the ligand donor atoms will decrease the strength of σ-bonding, accordingly red shift is also observed.

In the spectra of $[\{Cu(HL)\}_2] \cdot 2NO_3 \cdot nH_2O$ complexes, the d–d band appears at ca. 650 nm, implying the formation of five coordinate solvated species $[Cu(HLR)(DMF)_2]^{1+}$ [11].

3.5. *Magnetochemical studies*

Room-temperature magnetic moments of solid dichloro complexes, $[Cu(H_2LR)Cl_2] \cdot nH_2O$ (R = CH$_3$, OCH$_3$ and Cl), (1.88–1.91μ_B) are within the range reported for

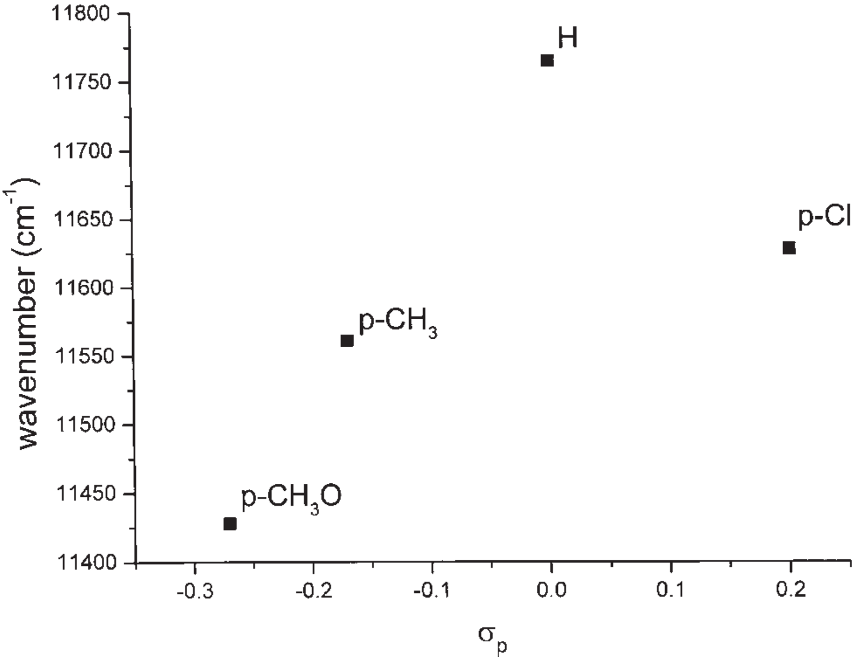

Figure 6. Plot of wavenumber (in cm^{-1}) of d–d transitions for dichloro complexes [Cu(H_2LR)Cl_2] against σ_p.

magnetically diluted copper(II) complexes [11]. Magnetic susceptibility measurements within the temperature range (4–300 K) suggest Curie–Weiss behaviour with Weiss temperature varies from -1.0 to -4.5 K, suggesting a monomeric structure as shown in figure 1 (structure **3**) [1].

Room temperature magnetic moments measured for both neutral, $[\{CuLR\}_2]\cdot nH_2O$ (figure 1, structure **2**, R = H, CH_3, CH_3O, Cl and NO_2), and nitrate complexes, $[\{Cu(HLR)\}_2]\cdot 2NO_3\cdot nH_2O$ (figure 1, structure **5**, (R = H, CH_3 and CH_3O), are significantly lower than the spin only value calculated for copper(II), indicating antiferromagnetic coupling between the copper(II) centres and suggest a dimeric structure for both neutral complexes and nitrate complexes [1, 13–15]. Variable temperature (4–300 K) magnetic susceptibility measurements were recorded for both neutral, $[\{CuLR\}_2]\cdot nH_2O$, and nitrate $[\{Cu(HLR)\}_2]\cdot 2NO_3\cdot nH_2O$ complexes and were fitted to a revised Bleaney–Bowers equation [16] (equation (1)) using isotropic (Heisenberg) exchange Hamiltonian ($H = -2JS_1\cdot S_2$) for two interacting $S = 1/2$ centres,

$$\chi_M = (1-\rho)\frac{2N_L\mu_B^2 g^2 \exp(2J/kT)}{k(T-\theta)[1+3\exp(2J/kT)]} + \rho\frac{2N_L\mu_B^2 g^2}{4kT} + 2N_\alpha \tag{1}$$

where χ_M is expressed per two copper(II) atoms, N_α is the temperature-independent paramagnetism [$60\times10^{-6}\,cm^3\,mol^{-1}$ per copper(II)], ρ is the fraction of monomeric impurity and θ is a correction term for interdimer interactions [17, 18]. A non-linear regression analysis was carried out with J, g, θ, and ρ as floating parameters and the

Table 5. The best-fit magnetic parameters for aroylhydrazoneoxime copper(II) complexes.

Complex						
R	*n*	μ_{eff} (μ_B) (298 K)	$-2J$ (cm^{-1})	*g*	θ (K)	ρ[a]
$[Cu(H_2LR)Cl_2]\cdot nH_2O$						
H		1.80	–	2.06	−3.5	–
p-CH_3		1.86	–	2.06	−4.0	–
p-CH_3O		1.88	–	2.06	−3.0	–
p-Cl		1.88	–	2.06	−3.1	–
$[\{Cu(LR)\}_2]\cdot nH_2O$						
H	1	0.76	757	2.08	−4.0	0.032
p-CH_3	2	0.77	780	2.08	−3.8	0.050
p-CH_3O	1	0.74	795	2.08	−3.8	0.032
p-Cl	2	0.87	700	2.08	−2.7	0.040
p-NO_2	3	0.84	630	2.08	−3.1	0.042
$[\{Cu(HLR)\}_2](NO_3)_2\cdot nH_2O$						
H	0	0.61	934	2.05	−4.0	0.020
p-CH_3	4	0.89	920	2.08	−3.1	0.139
p-CH_3O	2	0.63	940	2.08	−1.2	0.036

[a] The values of ρ given in reference 1 (table 3) are 100ρ and not the mole fraction ρ.

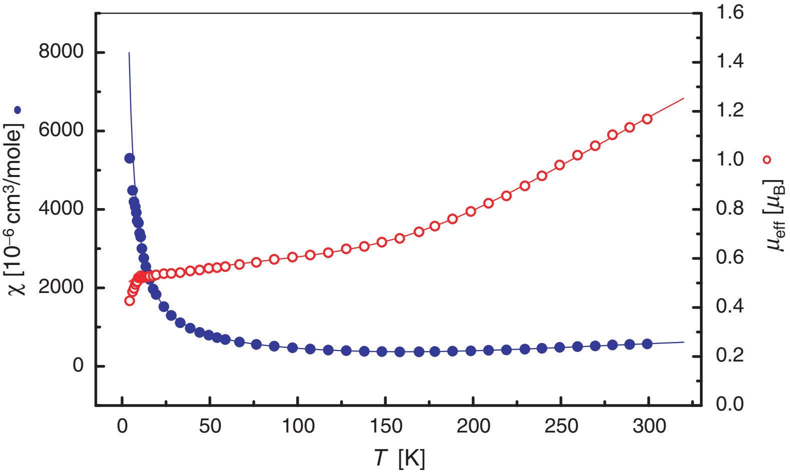

Figure 7. Magnetic susceptibilities χ_M (●) and magnetic moments μ_{eff} (○) vs. temperature for $[\{Cu(L\text{-}pNO_2C_6H_4\}_2]\cdot 3H_2O$. Solid lines represent the least-square fit to Bleaney–Bowers equation with $-2J = 639\,\mathrm{cm}^{-1}$, $g = 2.08$ and $\rho = 0.042$.

best-fit magnetic parameters ($-2J$, g, ρ and θ) are listed in table 5. The variation of molar magnetic susceptibility, χ_M, and magnetic moment, μ_{eff}, as a function of temperature for $[\{Cu(LNO_2)\}_2]\cdot 3H_2O$ and $[\{Cu(HLCH_3O)\}_2]\cdot 2NO_3\cdot 2H_2O$ are, respectively, given in figures 7 and 8. A similar profile was also observed for other neutral and nitrate copper(II) complexes. In all cases, the Neel maximum is higher than 300 K indicating strong antiferromagnetic coupling. The observed rise in susceptibility at low temperatures indicates the presence of small amount of paramagnetic impurity.

For neutral copper(II) complexes, $[\{CuLR\}_2]\cdot nH_2O$, the $-2J$ values, table 5, are within the range reported for other oximate bridged dicopper(II) complexes [13–15, 19–21] and show dependence on the nature of substituent in the aroylhydrazone

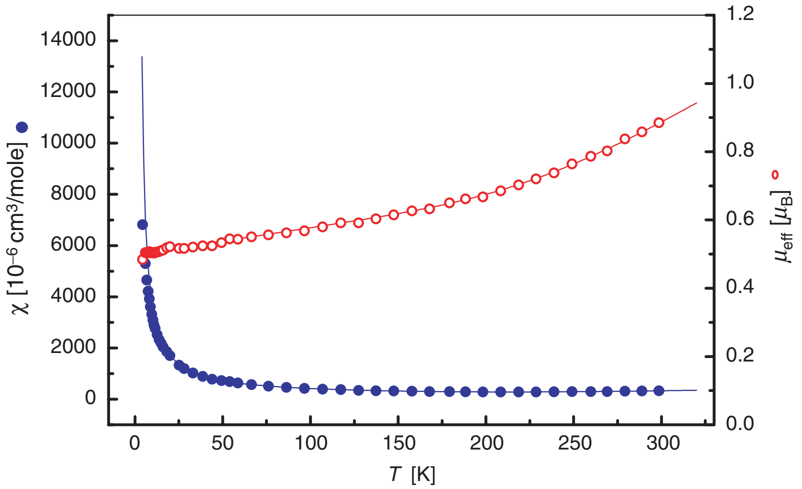

Figure 8. Magnetic susceptibilities χ_M (●) and magnetic moments μ_{eff} (○) vs. temperature for [{Cu(HL-pCH$_3$OC$_6$H$_4$}$_2$]·2NO$_3$·2H$_2$O. Solid lines represent the least-square fit to Bleaney–Bowers equation with $-2J = 940\,\mathrm{cm}^{-1}$, $g = 2.08$ and $\rho = 0.036$.

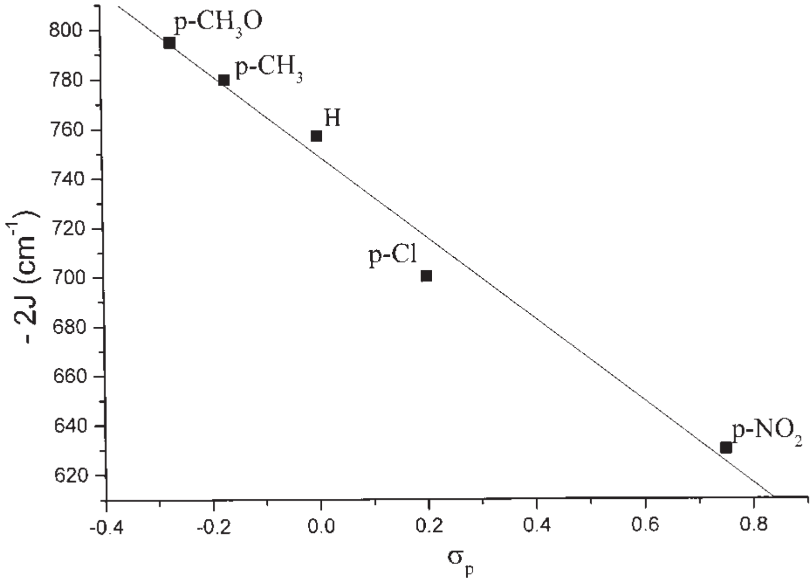

Figure 9. Plot of triplet–singlet separation ($-2J$) for neutral dimeric, [{Cu(LR)$_2$}], complexes against σ_p.

residue. Plot of $-2J$ values against Hammett's substituent constant (σ_p) is shown in figure 9. The observed linear correlation [correlation coefficient $(r) = 0.988$] suggests that all neutral dimeric complexes possess more or less similar structure and the observed variation in antiferromagnetic superexchange coupling can be related, mainly, to the electronic effect of the *p*-substituents in the aroylhydrazone residue which is transmitted to the oximate bridges via a highly delocalized π-framework. The negative slope indicates that the antiferromagnetic exchange coupling decreases with increasing σ_p value in agreement with Hoffmann's theoretical predictions [22]. Electron-releasing substituents (CH_3O and CH_3) will increase the electron density on the oximate bridging atoms, thus increasing antiferromagnetic interaction relative to the unsubstituted complex [22, 23]. The reverse effect was observed on introducing electron withdrawing substituents [24].

As previously reported [1], structure **5** (figure 1) can be tentatively proposed for the nitrate complexes. These nitrate complexes show higher ($-2J$) values relative to the corresponding neutral complexes in agreement with structure **5** (figure 1), where intramolecular hydrogen bonding stabilizes the planarity of the $Cu_2N_2O_2$ ring, thus allowing effective overlap between the oximate N–O orbitals and copper(II) $d_{x^2-y^2}$ orbital. It is of interest to note that the actual structure of the nitrate complexes must remain in doubt until X-ray molecular structure is available.

Acknowledgement

Thanks are due to BMBF/Forschungszentrm, Jüelich, ÖA-IB/Wo WTZ for supporting this bilateral project.

References

[1] M.F. Iskander, L. El Sayed, N.M.H. Salem, R. Werner, W. Haase. *J. Coord. Chem.*, **56**, 1075 (2003).
[2] M.F. Iskander, S.E. Zayan, M.A. Khalifa, L. El-Sayed. *J. Inorg. Nucl. Chem.*, **36**, 551 (1974).
[3] Sheffield Chemputer, Isotope Pattern. Available online at: www.shef.ac.uk/chemistry/isotopes.html
[4] S. Gehring, P. Fleichhauer, H. Paulus, W. Haase. *Inorg. Chem.*, **32**, 54 (1993).
[5] L. Walz, H. Paulus, W. Haase. *J. Chem. Soc., Dalton Trans.*, 913 (1985).
[6] A. Weiss, H. Witte. *MagnetoChemie*, Verlag Chemie, Weinheim (1973).
[7] M.M. Mostafa, M.A. Khattab, K.M. Ibrahim. *Synth. React. Inorg. Met. -Org. Chem.*, **14**, 39 (1984).
[8] M.M. Mostafa, K.M. Ibrahim, M.N.H. Moussa. *Trans. Met. Chem.*, **9**, 243 (1984).
[9] H. Okawa, M. Koikawa, S. Kida, D. Luneau, H. Oshio. *J. Chem. Soc., Dalton Trans.*, 469 (1990).
[10] T.-H. Lu, Y.-J. Lin, H. Luh, F.-L Liao, C.-S Chung. *Acta Cryst.*, **C57**, 1398 (2001); J.A. Bertrand, J.H. Smith, D.G. Van Der Veer. *Inorg. Chem.*, **16**, 1477 (1977).
[11] B.J. Hathaway. In *Comprehensive Coordination Chemistry*, G. Wilkinson, R.D. Gillard, J.A. McCleverty (Eds), Vol. 5, pp. 594–884, Pergamon Press, New York (1987).
[12] K.F. Purcell, J.C. Kotz. *Inorganic Chemistry*, pp. 533–559, W. B. Saunders Company, Philadelphia, PA (1977).
[13] M. Maekawa, S. Kitagawa, Y. Nakao, S. Sakamoto, A. Yatani, W. Mori, S. Kashino, M. Munakata. *Inorg. Chim. Acta*, **293**, 20 (1999).
[14] R.T. Butcher, C.J. O'Conner, E. Sinn. *Inorg. Chem.*, **18**, 1913 (1979).
[15] J.A. Bertrand, J.H. Smith, P.G. Eller. *Inorg. Chem.*, **13**, 1649 (1974).
[16] O. Kahn. *Molecular Magnetism*, VCH, New York (1993).
[17] K.T. McGregor, J.A. Barnes, W.E. Hatfield. *J. Am. Chem. Soc.*, **95**, 7993 (1973).
[18] S. Sikorav, I. Bkouche-Waksman, O. Kahn. *Inorg. Chem.*, **23**, 490 (1984).
[19] Y. Song, X.-T. Chen, C.-G. Zheng, D.-R. Zhu, X.Z. You, L.-H Weng. *Trans. Met. Chem.*, **26**, 247 (2001).
[20] J. Cano, A. Rodriguez-Fortea, P. Alemany, S. Alvarez, E. Ruiz. *Chem. Eur. J.*, **6**, 327 (2000).
[21] R. Ruiz, F. Lloret, M. Julve, M.C. Munoz, C. Bois. *Inorg. Chim. Acta*, **219**, 179 (1994).
[22] P.J. Hay, J.C. Thibeault, R. Hoffmann. *J. Am. Chem. Soc.*, **97**, 4884 (1975).
[23] H. OKawa, I. Ando, S. Kida. *Bull. Chem. Soc. (Japan)*, **47**, 3041 (1974)
[24] L.K. Thompson, S.K. Mandal, S.S. Tandon, J.N. Bridson, M.K. Park. *Inorg. Chem.*, **35**, 3117 (1996).